

# LIMNOLOGY and OCEANOGRAPHY



© 2020 Association for the Sciences of Limnology and Oceanography doi: 10.1002/lno.11668

# Trophic ecology of Caribbean sponges in the mesophotic zone

Keir J. Macartney , 1\* Marc Slattery, 2 Michael P. Lesser 101

<sup>1</sup>Department of Molecular, Cellular and Biomedical Sciences and School of Marine Science and Ocean Engineering, University of New Hampshire, Durham, New Hampshire

# **Abstract**

Sponges are a crucial component of Caribbean coral reef ecosystem structure and function. In the Caribbean. many sponges show a predictable increase in percent cover or abundance as depth increases from shallow (< 30 m) to mesophotic (30-150 m) depths. Given that sponge abundances are predicted to increase in the Caribbean as coral cover declines, understanding ecological factors that control their distribution is critical. Here we assess if sponge cover increases as depth increases into the mesophotic zone for three common Caribbean reef sponges, Xestospongia muta, Agelas tubulata, and Plakortis angulospiculatus, and use stable isotope analyses to determine whether shifts in trophic resource utilization along a shallow to mesophotic gradient occurred. Ecological surveys show that all target sponges significantly increase in percent cover as depth increases. Using bulk stable isotope analysis, we show that as depth increases there are increases in the  $\delta^{13}$ C and  $\delta^{15}$ N values, reflecting that all sponges consumed more heterotrophic picoplankton, with low C:N ratios in the mesophotic zone. However, compound-specific isotope analysis of amino acids (CSIA-AA) shows that there are speciesspecific increases in  $\delta^{13}C_{AA}$  and  $\delta^{15}N_{AA}$  values. Xestospongia muta and P. angulospiculatus showed a reduced reliance on photoautotrophic resources as depth increased, while A. tubulata appears to rely on heterotrophy at all depths. The  $\delta^{13}C_{AA}$  and  $\delta^{15}N_{AA}$  values of these sponges also reflect species-specific patterns of host utilization of both POM and dissolved organic matter (DOM), its subsequent re-synthesis, and translocation, by their microbiomes.

As coral reefs around the world continue to show declines in biodiversity and health (Hoegh-Guldberg et al. 2007; Hughes et al. 2017, 2018) there has been increased interest in understanding processes affecting the structure and function of coral reef communities in the Anthropocene (Waters et al. 2016). The decline in coral cover due to anthropogenic stressors such as pollution, ocean acidification and increases in sea surface temperature (e.g., Hoegh-Guldberg et al. 2007) has resulted in ecological phase shifts in the benthic communities of many coral reefs (McManus 2000). These community shifts are predicted to cause an increase in the abundance of sponges, and changes in the functional attributes of coral reefs as sponge biomass exceeds coral biomass Caribbean-wide (McMurray et al. 2010; Bell et al. 2013, 2018). In the Caribbean, sponges provide an important source of food and habitat for a variety of coral reef species (Diaz and Rützler 2001; Bell 2008). Sponges also play an important role in benthic food webs through benthic-pelagic coupling due to their consumption of live particulate organic material (POM) (Pile

Additional Supporting Information may be found in the online version of this article.

et al. 1997; Lesser 2006; Lesser and Slattery 2013) and dissolved organic material (DOM) (de Goeij et al. 2013, 2017; Mueller et al. 2014), thus coupling water column productivity to benthic secondary productivity (Gili and Coma 1998; Lesser 2006).

While many ecological studies on the trophic ecology of sponges have been conducted on shallow coral reefs (de Goeij et al. 2017), studies in the mesophotic zone, while increasing (Loya et al. 2016), are not as common (Lesser et al. 2018). The mesophotic zone is found between 30 and 150 m and is defined primarily by gradients of abiotic factors, particularly irradiance (Lesser et al. 2018). Along the shallow to mesophotic depth gradient, sponges exhibit increased growth rates, abundances, and diversity (Lesser 2006; Trussell et al. 2006; Lesser and Slattery 2013; Slattery and Lesser 2015). Additionally, their primary particulate food sources, auto- and heterotrophic picoplankton, increase with depth (Lesser 2006; Lesser and Slattery 2013). As sponges consume particulate and dissolved food in proportion to its availability (Lesser 2006; de Goeij et al. 2008; Slattery and Lesser 2015), mesophotic sponges should therefore consume more POM with increasing depth (e.g., Slattery and Lesser 2015). Despite the fact that dissolved organic carbon (DOC) declines with increasing depth

<sup>&</sup>lt;sup>2</sup>Department of BioMolecular Science, University of Mississippi, Oxford, Mississippi

<sup>\*</sup>Correspondence: kjm1049@wildcats.unh.edu

(Lesser et al. 2019), it has been suggested that carbon, including both particulate organic carbon (POC) and DOC, is not limiting for sponges along the shallow to mesophotic depth range (Lesser et al. 2018, 2020; Lesser and Slattery 2018). Nitrogen, however, is much more likely to be a limiting nutrient for sponge growth (e.g., Hadas et al. 2009). Heterotrophic picoplankton, with low C:N ratios, increase significantly in abundance with increasing depth and may supply the nitrogen required for the increased growth rates and biomass of mesophotic sponges (Lesser et al. 2018). These patterns suggest that sponge populations along the shallow to mesophotic depth gradient are strongly influenced by bottom-up processes (Slattery and Lesser 2015; de Goeij et al. 2017; Wulff 2017; Lesser et al. 2018).

One of the most common analytical tools used for studying the trophic ecology of an organism is bulk stable isotopic analysis (SIA), particularly the stable isotopes  $\delta^{15}N$  and  $\delta^{13}C$ (Fry 2006). However, sponges present a unique problem for SIA-based studies of their trophic ecology due to the presence of a diverse microbiome in their tissues and their consumption of free-living microbes in the plankton (Hentschel et al. 2012; Pita et al. 2018). For sponges, the bulk  $\delta^{13}$ C and  $\delta^{15}$ N values increase as depth increases into the mesophotic zone (Slattery et al. 2011; Morrow et al. 2016), indicating a shift in diet from autotrophic to heterotrophic resources at mesophotic depths. Using compound-specific isotope analysis of amino acids (CSIA-AA) may provide increased resolution, compared to bulk SIA, of sponge trophic ecology along environmental gradients. Because of the unique fractionation patterns for stable isotopes of C and N for amino acids (AAs), the  $\delta^{13}$ C of essential amino acids (EAAs) can be used to effectively "fingerprint" the biosynthetic origin of source carbon due to the highly conserved modes of carbon acquisition in bacteria, algae and fungi as the δ<sup>13</sup>C of these EAA is maintained throughout the food web due to low fractionation between trophic levels (Larsen et al. 2009, 2013; McMahon et al. 2016), which allows for predictions of source end-members utilized by the consumer (Larsen  $\delta^{15} N \,$ 2013). The composition (e.g., phenylalanine) vs "trophic" (e.g., glutamic acid) AAs are informative for both the estimation of trophic position (TP) and the  $\delta^{15}$ N composition of AAs at the base of the food web. Source AAs (SAA) undergo minimal to no fractionation as they are transferred through a food web (Phe =  $\sim 0.5\%$ ) (Chikaraishi et al. 2009) and thus reflect the biosynthetic origin of that SAA, whereas the  $\delta^{15}N$  of trophic AAs (TAA) increase by as much as  $\sim 7-8\%$  per trophic level (McClelland and Montoya 2002; Chikaraishi et al. 2009; McMahon et al. 2015). Additionally,  $\Sigma V$  values, a measure of bacterial resynthesis and translocation of organic matter, have been successfully used to understand the interactions between the sponge host and its microbiome (Shih et al. 2020).  $\Sigma V$  values assess the reliance of sponges on translocated organic material vs. feeding from the water column and will be applied here using the CSIA-AA data on sponges from shallow to mesophotic depths.

muta **Plakortis** Agelas tubulata, Xestospongia and angulospiculatus are three common sponges on coral reefs throughout the Caribbean, and are all classified as high microbial abundance (HMA) sponges (Gloeckner et al. 2014). While HMA sponges are known to filter feed upon picoplankton (e.g., Lesser 2006) it is generally accepted that because of their high microbial densities they efficiently utilize DOM as well (Maldonado et al. 2012). Here we assess if the percent cover of these three sponge species increases as depth increases into the mesophotic zone on Little Cayman Island, and use SIA and CSIA-AA to quantify shifts in trophic resource utilization along a shallow to mesophotic depth gradient. We hypothesize that these sponges will increase in cover with increasing depth and rely upon the increasing concentration of available POM with increasing depth and this will be reflected in their isotopic signatures. Additionally, variability in the utilization of DOM by the sponge microbiome with depth will affect the transfer of resynthesized organic material to the host, which will be reflected in reductions in the  $\Sigma V$  values of these sponges.

#### Materials and methods

# Target sponge abundance surveys, sample collection and processing

Replicate samples (n = 3) of A. tubulata, X. muta and P. angulospiculatus were collected using open circuit technical diving at 10, 18, 30, 61, and 91 m at Rock Bottom Wall, Little Cayman, Cayman Islands (19° 42′7.36″N, 80° 3′24.94″W) in the Spring of 2009. The abiotic environment (i.e., light, temperature) of this site from shallow to mesophotic depths is described in Morrow et al. (2016), while from an oceanographic perspective this site is occasionally impacted by internal waves (Lesser et al. 2009). To quantify sponge cover with increasing depth the percent cover of the target species was estimated using replicate (n = 10) 1 m<sup>2</sup> quadrats positioned at random points along transect lines (n = 3-9 at each depth) of  $20 \times 2$  m at each depth. The survey data for P. angulospiculatus presented are from Slattery et al. (2016) and reanalyzed for this study. At each depth, all sponges were sampled by cutting a "pie-slice" of sponge tissue from the apical lip of the osculum including both pinacoderm and mesohyl as described in Morrow et al. (2016). Samples were transported on ice to the laboratory and immediately frozen. All samples were transported frozen to the University of New Hampshire where they were freeze-dried and ground to a powder for stable isotope analyses.

#### Bulk stable isotope analysis

Bulk stable isotope data for *X. muta* were taken from Morrow et al. (2016), and for *A. tubulata* the data are from Slattery et al. (2011) and reanalyzed here to compare to the CSIA-AA analyses. For *P. angulospiculatus*, subsamples from each piece of sponge tissue, sampled as described above, were sent to the Marine Biological Laboratory (Woods Hole, MA) for the bulk analysis of particulate C and N, as well as the natural abundance

of the stable isotopes  $\delta^{15}N$  and  $\delta^{13}C$ . Samples were analyzed using a Europa ANCA-SL elemental analyzer-gas chromatograph attached to a continuous-flow Europa 20-20 gas source stable isotope ratio mass spectrometer. The carbon isotope results are reported relative to Vienna Pee Dee Belemnite, nitrogen isotope results are reported relative to atmospheric air, and both are expressed using the delta  $(\delta)$  notation in units per mil  $(\infty)$ .

#### Compound specific isotope analysis of amino acids

Sponge samples were sent to the Isotope Biogeochemistry Laboratory at the University of Hawai'i at Manoa for  $\delta^{15}N$  and  $\delta^{13}$ C analysis of individual amino acids. Both  $\delta^{15}$ N and  $\delta^{13}$ C, were quantified using gas chromatography/combustion-isotope ratio mass spectrometry (GC/C-IRMS) after amino acid extraction and derivatization. Samples were analyzed using either a Thermo Scientific Delta V Plus or a Thermo Scientific MAT 253 mass spectrometer interfaced with a Thermo Finnigan Trace GC gas chromatograph via a Thermo Finnigan GC-C III. The amino acids measured using this technique were alanine (Ala), glycine (Gly), threonine (Thr), serine (Ser), valine (Val), leucine (Leu), isoleucine (Iso), proline (Pro), aspartic acid (Asp), phenylalanine (Phe), and lysine (Lys). The terminal amide groups in glutamine (Gln) and aspartame (Asn) were cleaved during the chemical isolation of amino acids. This resulted in the conversion of these amino acids to glutamic acid (Glu) and aspartic acid (Asp), respectively. Thus, the isotope value of the combined Glu + Gln was measured (termed Glx), and the isotope value of a combined Asn + Asp was measured (termed Asx). Averaged AA  $\delta^{13}$ C and  $\delta^{15}$ N values from these analyses can be found in Tables S1 and S2, while additional information on CSIA is available in the supplemental document.

#### Statistical analyses

Statistical analyses were conducted using PRIMER (version 7) or JMP (v. 14), and R (version 3.4.3). Differences in percent cover of sponges as a function of depth was assessed with linear regression. Differences in bulk SIA values between species were assessed using ANOVA, and differences between SIA values along the depth gradient were assessed using linear regression.

The  $\delta^{13}C$  values of each amino acid in all sponge samples were normalized to the mean value of all AAs in the sample ( $\delta^{13}C_{norAA}=\delta^{13}C_{AA}$  [of interest]-mean all AAs in sample) as described for the multivariate statistics required for the  $\delta^{13}C$  fingerprinting approach described in Larsen et al. (2013). To assess if CSIA-AA can be used to separate bacterial isotopic values from sponge isotopic values, a principal component analysis (PCA) and linear discriminant analysis (LDA) were conducted on  $\delta^{13}C_{norEAA}$  from the sponges at each depth using source end-member data from Larsen et al. (2013) and McMahon et al. (2016). It should be noted that the end-member source data used in these analyses while not depth-dependent, represent the best available data for invertebrates and their food sources, including representatives from coral reefs.

Differences in the mean of all  $\delta^{13}C_{AA/EAA}$  and  $\delta^{15}N_{AA/SAA/TAA}$ . TP, and  $\Sigma V$  values between depths within each species were assessed using linear regression with depth as a continuous variable (significance level of  $\alpha=0.05$ ). Differences in mean  $\delta^{13}C_{AA/EAA}$  and  $\delta^{15}N_{AA/SAA/TAA}$ , TP, and  $\Sigma V$  values between species were also assessed using ANOVA (ANOVA) with Tukey HSD post hoc tests as needed (significance level of  $\alpha=0.05$ ). Any data not meeting the assumptions of normality were log-transformed before analyses. The trophic position of sponges at each depth was calculated with  $\delta^{15}N_{Phe}$  and  $\delta^{15}N_{Glx}$  using a sponge species-specific enrichment factor calculated as described in Chikaraishi et al. (2014) using the formula:

$$TP_{Glx/Phe} = \left[ \left( \delta^{15} N_{Glx} - \delta^{15} N_{Phe} + \beta \right) / TDF \right] + 1$$

where  $\beta$  represents the isotopic difference between  $\delta^{15}N_{Glu}$  and  $\delta^{15}N_{Phe}$  in aquatic cyanobacteria and algae (– 3.4 – 0.9). Species-specific discrimination factors (TDF) were calculated by subtracting the mean  $\delta^{15}N_{SAA}$  from the mean  $\delta^{15}N_{TAA}$  of each sponge, then the mean value of that calculation from each set of samples was calculated for use as the species-specific discrimination factor (*X. muta* = 8.077, *P. angulospiculatus* = 7.318, *A. tubulata* = 4.75). The  $\Sigma V$  value was calculated as outlined in McCarthy et al. (2007) and as described by Shih et al. (2020), using the average deviation of seven trophic  $\delta^{15}N_{AA}$  values (Ala, Glu, Leu, Iso, Pro, Asx, Glx) for all samples as follows:

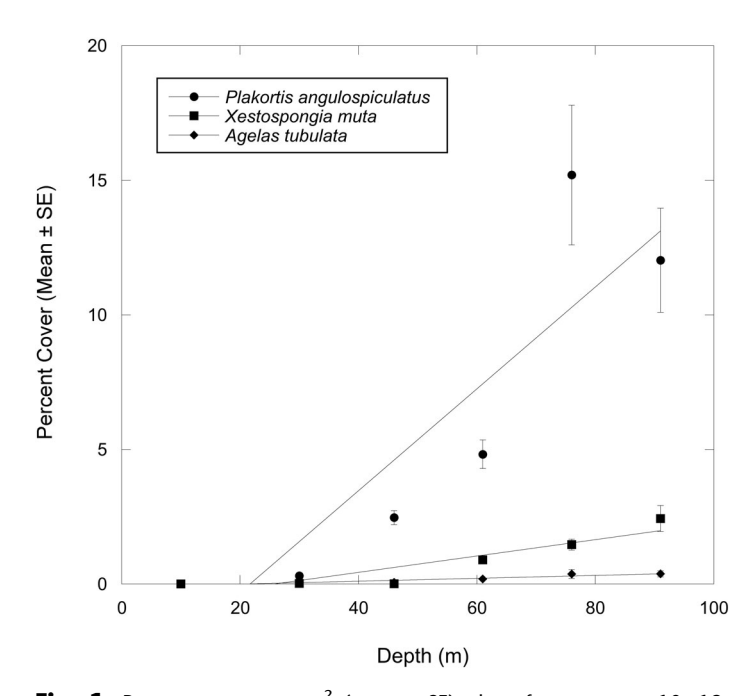


**Fig. 1.** Percent cover per m<sup>2</sup> (mean  $\pm$  SE) plot of sponges at 10, 18, 30, 61, and 91 m. Regression analysis for effect of depth were all significant: *Plakortis angulospeculatus*, y = -4.0968 + 0.18922x,  $R^2 = 0.787$  (t [28] = 8.61,  $p \le 0.0001$ ), A. tubulata, y = -0.1105 + 0.0054x,  $R^2 = 0.893$  (t[28] = 6.50,  $p \le 0.0001$ ), X. muta, y = -0.7867 + 0.0305x,  $R^2 = 0.831$  (t [28] = 8.60,  $t \le 0.0001$ ).

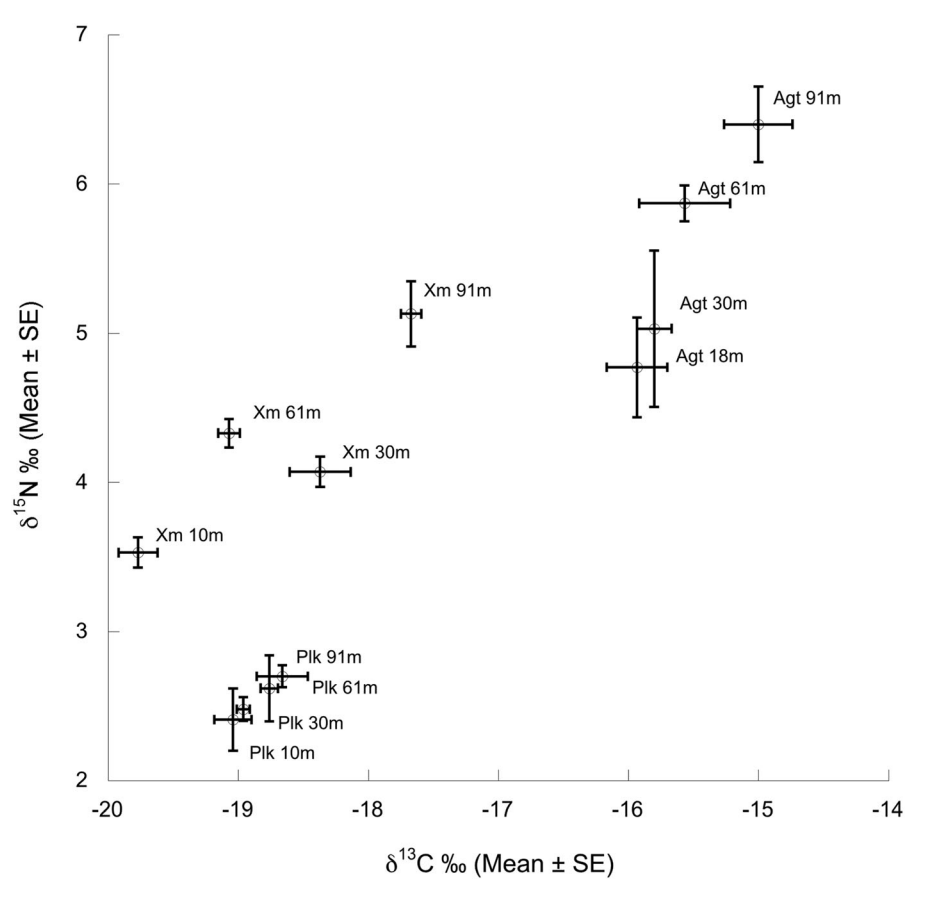


**Fig. 2.** Bivariate plot of bulk stable isotope data for  $\delta^{13}$ C and  $\delta^{15}$ N from *X. muta* (Xm), *P. angulospiculatus* (Plk), and *A. tubulata* (Aqt).

$$\Sigma V = 1/n \Sigma \text{Abs}(X_{AA})$$

where *X* of each trophic AA =  $(\delta^{15}N_{AA} - AVG \delta^{15}N_{AA})$  (Ala, Glu, Leu, Iso, Pro, Asx, Glx)), and n = the total number of  $\delta^{15}N_{AA}$  used in the calculation.

# Results

#### Sponge environment and survey results

From Morrow et al. (2016) vertical profiles of PAR for Little Cayman showed that the maximum surface irradiances were  $\sim 2400~\mu mol$  quanta  $m^{-2}~s^{-1}.$  With a  $K_{dPAR}$  for the water

**Table 1.** Means (± SE) of Bulk  $\delta^{13}$ C, Bulk  $\delta^{15}$ N,  $\delta^{13}$ C<sub>EAA</sub>,  $\delta^{15}$ N<sub>SAA</sub>,  $\delta^{15}$ N<sub>TAA</sub>, trophic position (TP) and  $\Sigma V$  value data for the target species and all depths.

Species	Depth (m)	Bulk δ <sup>13</sup> C (± SE)	Bulk δ <sup>15</sup> N (± SE)	δ <sup>13</sup> C <sub>EAA</sub> (± SE)	δ <sup>15</sup> N <sub>SAA</sub> (± SE)	δ <sup>15</sup> N <sub>TAA</sub> (± SE)	TP phe- glu (± SE)	ΣV value (± SE)
X. muta	10	-19.77 (0.15)	3.53 (0.10)	-19.96 (0.53)	0.11 (0.21)	8.85(0.28)	2.03 (0.10)	1.65(0.04)
X. muta	30	-19.07 (0.08)	4.33 (0.09)	-19.41 (0.37)	-0.04 (0.44)	8.91 (0.95)	1.96 (0.19)	1.77 (0.01)
X. muta	61	-18.37 (0.23)	4.07 (0.10)	-19.73 (0.11)	0.74 (0.09)	8.79 (0.49)	1.85 (0.04)	1.43 (0.03)
X. muta	91	-17.67 (0.07)	5.13 (0.21)	-18.89 (0.33)	2.36 (0.29)	9.72 (0.21)	1.86 (0.05)	1.86 (0.01)
A. tubulata	18	-15.93 (0.23)	4.77 (0.33)	-19.48 (0.47)	1.40 (0.21)	5.96 (0.13)	1.74 (0.05)	0.85 (0.11)
A. tubulata	30	-15.80 (0.13)	5.03 (0.52)	-18.8 (0.25)	1.7 (0.28)	6.20 (0.35)	1.75 (0.10)	0.82 (0.11)
A. tubulata	61	-15.56 (0.35)	5.87 (0.12)	-18.92 (0.10)	2.175 (0.21)	6.89 (0.41)	1.90 (0.12)	0.98 (0.12)
A. tubulata	91	-15.00 (0.26)	6.40 (0.25)	-18.1 (1.16)	1.2 (0.57)	6.43 (0.31)	1.96 (0.19)	0.94 (0.08)
P. angulospiculatus	10	-19.04 (0.14)	2.41 (0.21)	-19.12 (0.21)	-1.23 (0.59)	5.61 (0.25)	1.66 (0.02)	1.47 (0.07)
P. angulospiculatus	30	-18.96 (0.05)	2.48 (0.08)	-19.75 (0.14)	0.133 (0.24)	6.69 (0.50)	1.56 (0.02)	1.5 (0.05)
P. angulospiculatus	61	-18.76 (0.06)	2.62 (0.22)	-18.83 (0.35)	-0.55 (0.33)	6.98 (0.16)	1.40 (0.23)	1.48 (0.08)
P. angulospiculatus	91	-18.66 (0.19)	2.70 (0.07)	-17.71 (0.16)	-0.175 (0.44)	8.15 (0.08)	1.63 (0.23)	1.79 (0.09)

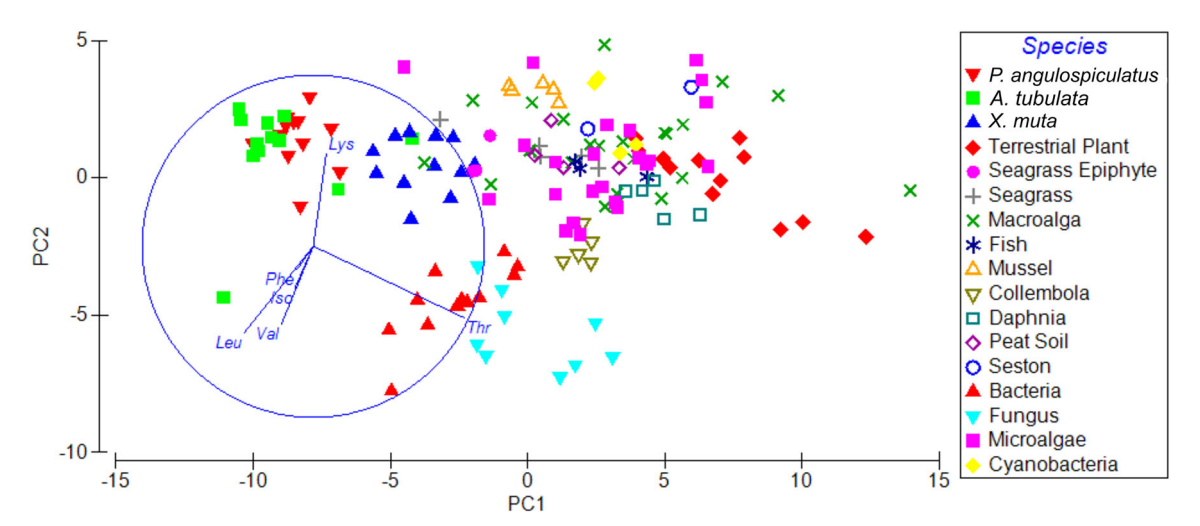


**Fig. 3.** Fingerprinting method for separating functional groups based on principal component analysis of CSIA  $\delta^{13}C_{norEAA}$  data. Sponge  $\delta^{13}C_{norEAA}$  values are unique, species-specific and well separated compared to potential food resources of prokaryotic and eukaryotic origin, as well as other filter feeding organisms (e.g., mussels).

column that ranged from 0.056 to 0.057 m $^{-1}$ . Vertical profiles of temperature showed a temperature of  $\sim 28.5^{\circ}$ C at the surface and  $\sim 24.5^{\circ}$ C at 91 m. For the percent cover of sponges with depth a significant increase was observed for *X. muta, A. tubulata* and *P. angulospiculatus* (Fig. 1) with the largest increase in percent cover coming at, or after,  $\sim 60$  m depth for all species.

## Bulk stable isotope analyses

The bulk stable isotopes of the three sponges show species-specific differences but all show a pattern of increasing values with increasing depth into the mesophotic zone (Fig. 2, Table 1). There were significant differences between all species in tissue  $\delta^{13}$ C (ANOVA: F=63.1331,  $p \le 0.0001$ , Tukey's HSD:  $p \le 0.05$ ), and  $\delta^{15}$ N (ANOVA: F=53.996,  $p \le 0.0001$ , Tukey's HSD:  $p \le 0.05$ ). There was also a significant effect observed, using regression analyses of the data in Table 1, for depth on the bulk tissue  $\delta^{13}$ C (t[10]=6.39,  $p \le 0.0001$ ) and  $\delta^{15}$ N (t[10]=3.07, p=0.012) for x. muta, a. tubulata  $\delta^{13}$ C (t[10]=4.20, p=0.001) and  $\delta^{15}$ N (t[10]=4.21, t[10]=0.001) and t[10]=0.0010 and t[10]=0.0011 and t[10]=0.0012 and t[10]=0.0013 and t[10]=0.0013 and t[10]=0.0014.

# Compound specific isotope analyses of amino acids

The  $\delta^{13}C_{EAA}$  fingerprinting analysis, using the Larsen et al. (2013)  $\delta^{13}C_{EAA}$  training data set, showed that sponges' group separately from most other organisms, but by sponge species (Fig. 3). In both analyses, sponges with known symbionts are differentiated from their potential food sources such as microalgae, fungus, and bacteria, with microalgae grouping closely with macroalgae. The LDA was used to assess biosynthetic origin of sponge carbon, and the LDA predicted potential end-member groups with 91% accuracy. All sponges are primarily classified with bacteria, detritus, microalgae or

macroalgae but not POM (plankton collection using 5  $\mu$ m mesh net) (Fig. 4).

To quantify changes in trophic strategy between depths, an ANOVA was used on species and linear regression was applied to the mean values of all  $\delta^{13}C_{EAA}$ ,  $\delta^{15}N_{SAA}$ ,  $\delta^{15}N_{TAA}$ , TP, and  $\Sigma V$  measurements between depths for each species (Table 1, Fig. 5). There were no significant differences in  $\delta^{13}C_{EAA}$ between species (ANOVA: F = 2.2217, p = 0.124). There were significant differences in  $\delta^{15}N_{SAA}$  (ANOVA: F = 17.1226,  $p \le 0.0001$ ) with P. angulospiculatus significantly lower than both X. muta and A. tubulata (Tukey's HSD: p < 0.05) and significant differences in  $\delta^{15}N_{TAA}$  (ANOVA: F = 32.403,  $p \leq 0.0001$ ), with X. muta significantly greater than *P. angulospiculatus* and *A. tubulata* (Tukey's HSD:  $p \le 0.05$ ). Significant differences were detected (ANOVA: F = 11.432, p = 0.0002) in TP between species with P. angulospiculatus significantly lower than A. tubulata and X. muta (Tukey's HSD: p = <0.05). There were significant differences between species for  $\Sigma V$  values, with higher values indicating more microbial repossessing and translocation of organic matter to the host (ANOVA: F = 69.702,  $p \le 0.0001$ ). Post-hoc comparisons revealed that A. tubulata  $\Sigma V$  values were significantly lower than X. *muta* and *P. angulospiculatus* (Tukeys HSD:  $p \le 0.05$ ) (Table 1).

Using regression analysis there was no significant effect of depth on  $\delta^{13}C_{EAA}$  ( $t[10]=1.73,\ p=0.114$ ),  $\delta^{15}N_{TAA}$  ( $t[10]=1.08,\ p=0.305$ ), TP ( $t[10]=-1.29,\ p=0.225$ ) or  $\Sigma V$  value ( $t[10]=0.63,\ p=0.541$ ) for X. muta (Table 1). But there was a significant effect of depth on  $\delta^{15}N_{SAA}$  ( $t[10]=4.97,\ p\leq0.0001$ ) (Table 1). For A. tubulata there was no significant effect of depth on  $\delta^{13}C_{EAA}$  ( $t[10]=1.51,\ p=0.163$ ),  $\delta^{15}N_{SAA}$  ( $t[10]=-0.18,\ p=0.864$ ),  $\delta^{15}N_{TAA}$  ( $t[10]=1.38,\ p=0.197$ ), TP ( $t[10]=1.61,\ p=0.138$ ) or  $\Sigma V$  value ( $t[10]=0.99,\ p=0.3471$ ) (Table 1). For P. angulospiculatus there was no significant effect of depth on  $\delta^{15}N_{SAA}$  ( $t[10]=1.02,\ p=0.332$ ) or TP (t

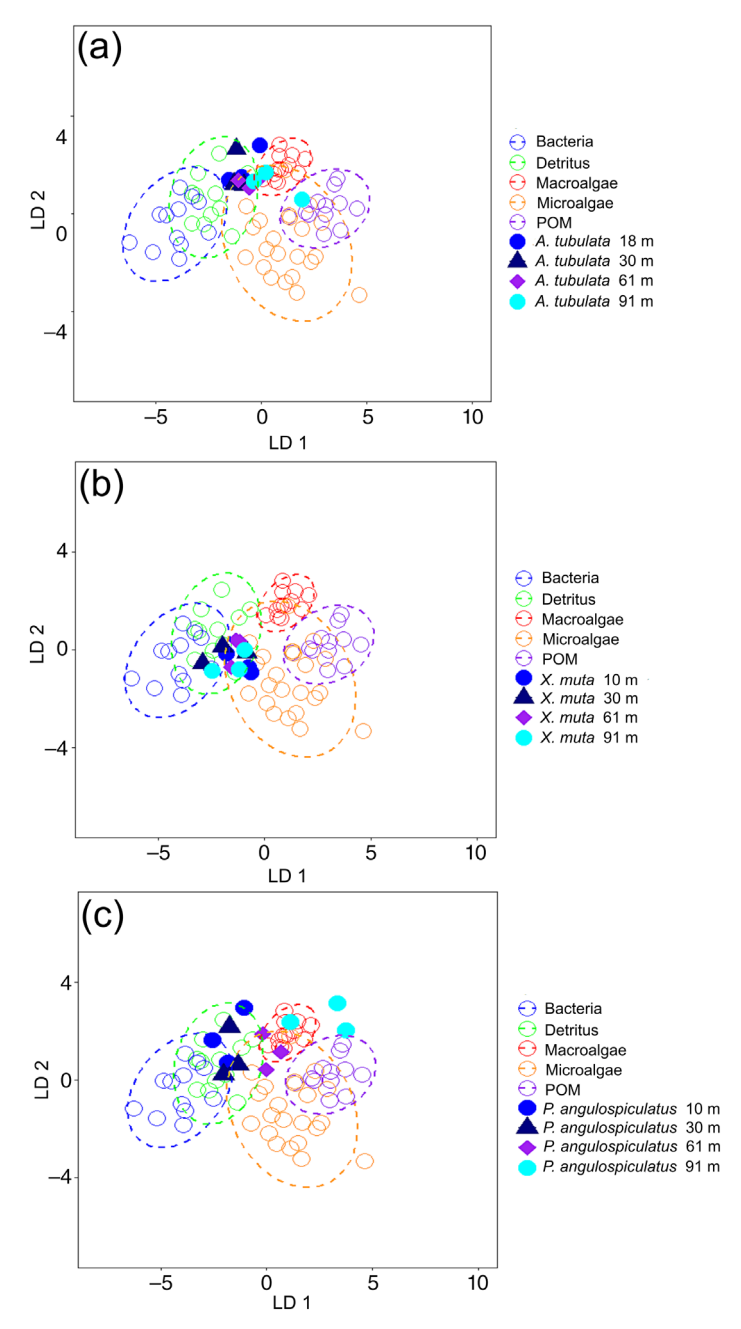


**Fig. 4.** Linear discriminant analysis plots from CSIA  $\delta^{13}C_{norEAA}$  data from a) *A. tubulata* B) *X. muta* and C) *P. angulospiculatus*. Source end member data was taken from the Larsen et al. (2013) CSIA  $\delta^{13}C_{norEAA}$  and from McMahon et al. (2016).

[10] = -0.41, p = 0.689), while there was a significant effect of depth on  $\delta^{13}C_{EAA}$  (t[10] = 3.71, p = 0.004),  $\delta^{15}N_{TAA}$  (t[10] = 5.78, p = 0.001), and  $\Sigma V$  value (t[10] = 2.55, p = 0.0287) (Table 1).

## Discussion

The sponge species used for this study show an increase in percent cover from shallow to mesophotic depths in Little

Cayman consistent with sponges from multiple locations in the Caribbean (Lesser and Slattery 2018), and the Pacific (Slattery and Lesser 2012; Lesser and Slattery 2018). The increase in sponge cover also occurs at the beginning of the lower mesophotic ( $\sim 60 \text{ m}$ ) and is consistent with recent observations of global faunal breaks for mesophotic taxa on coral reefs (Lesser et al. 2019). Sponge cover increases with depth (Fig. 1), and are known to grow faster and have increased scope for growth as depth increases in the Caribbean at both shallow and mesophotic depths (Lesser 2006; Trussell et al. 2006; Lesser and Slattery 2018). Previous studies have shown this pattern to be associated with increased particulate trophic resources available to them as depth increases (Lesser 2006; Slattery et al. 2011; Lesser et al. 2019, 2020). Specifically, particulate nitrogen availability increases with depth (Lesser et al. 2019, 2020) and may play a key role in the patterns of sponge distribution in the Caribbean mesophotic zone (de Goeii et al. 2017).

The bulk SIA data from the three sponges in this study shows a species-specific pattern as depth increases (Fig. 2). The  $\delta^{13}$ C values reflect the consumption of both photoautotrophically produced DOM and photoautotrophic and heterotrophic POM (Table 1,  $\delta^{13}$ C marine picoplankton: -19 to -24‰, DOM: -16 to -23‰) (Fry 2006; Slattery et al. 2011; Hansell and Carlson 2014; van Duyl et al. 2011; 2018), as well as fractionation processes, such as carbon or nitrogen cycling, and photoautotrophy, facilitated by the species-specific microbiomes of these sponges. The data show that heterotrophy increases with increasing depth as lighter isotopes are favored during waste excretion leading to an increase in  $\delta^{15}N$ values at higher trophic levels (i.e., more of the heavier isotope leads to an increase in  $\delta^{15}N$  values). The increases in both  $\delta^{13}$ C and  $\delta^{15}$ N suggest an increased, and proportional, reliance on heterotrophic picoplankton as photoautotrophic picoplankton declines into the mesophotic zone as reported previously (Lesser 2006; Trussell et al. 2006; Slattery et al. 2011).

Analyses of the CSIA-AA data, using the  $\delta^{13}C_{norEAA}$  fingerprinting method based on the Larsen et al. (2013) training dataset and data from McMahon et al. (2016), reveals that sponge δ<sup>13</sup>C<sub>norEAA</sub> values are both unique to sponges and species-specific when compared to the  $\delta^{13}C_{norEAA}$  of a wide range of both prokaryotic and eukaryotic organisms (Fig. 3). Sponges were unambiguously separated from their principal planktonic food sources such as cyanobacteria and free-living bacteria (Fig. 3). This was possible despite the fact that sponges host a microbiome consisting of these groups in their tissues. This suggests fundamental differences in the microbial communities of sponges vs. the bacterioplankton of the surrounding seawater that can be distinguished using CSIA-AA. For instance, there are multiple aerobic or anaerobic microenvironments within a sponge (Fiore et al. 2010) that are linked to the metabolic diversity found in sponge microbiomes (Hentschel et al. 2012; Fiore et al. 2015; Pita et al. 2018). A

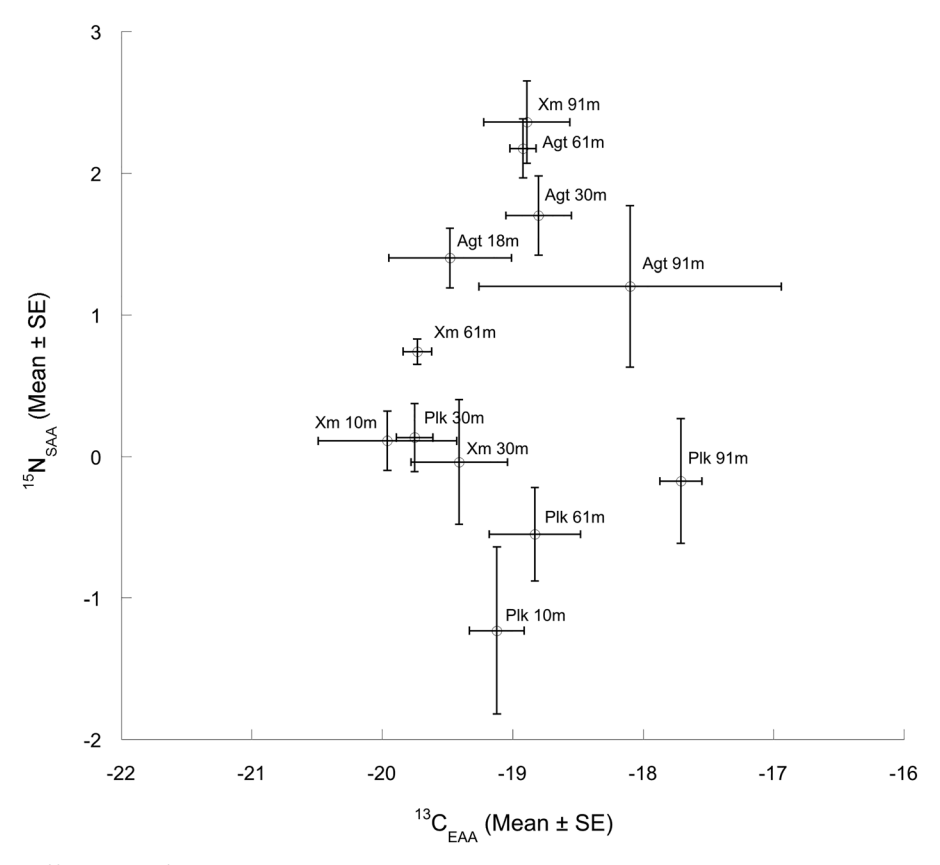


**Fig. 5.** Bivariate plot of CSIA  $\delta^{13}C_{EAA}$  and  $\delta^{15}N_{SAA}$  stable isotope data from *X. muta* (Xm), *P. angulospiculatus* (Plk) and *A. tubulata* (Agt).

wide range of  $\delta^{13}C_{norEAA}$  values from these metabolic pathways could be contributing to the observed ability to discriminate between the sponge microbiome and the ambient bacterioplankton communities.

An LDA (Fig. 4) of  $\delta^{13}C_{norEAA}$  was used to assess the source end-member each sponge sample classified most closely with, based on data from Larsen et al. (2013) and McMahon et al. (2016). All sponges classify most closely with bacteria, detritus and macroalgae (a proxy for DOM), suggesting a reliance on a mixed diet of POM and DOM at all depths. The LDA also reveals patterns that are likely a result of the speciesspecific microbiomes utilization of DOM and in the case of X. muta, a loss of cyanobacterial photosynthate due to reductions in available PAR, or reductions in cyanobacterial symbiont abundances with depth (Morrow et al. 2016). This is also seen in the significant increases in the bulk  $\delta^{13}$ C and the trend of increases in the  $\delta^{13}C_{EAA}$ , indicating potential reductions in carbon fixed via photoautotrophy as depth increases. The DOM consumed by sponges could be used for microbial production of essential amino acids, as essential amino acids are derived from microbial, algal or plant organic material and cannot be synthesized de novo in animals (Larsen et al. 2009, 2013; McMahon et al. 2016). The microbiome may then translocate (sensu Fiore et al. 2015; Shih et al. 2020) specific nutrients to the host or be consumed directly through phagocytosis (sensu Leys et al. 2018) to be used for sponge growth. It is evident that DOM is an important component of the diets of the sponge holobiont but as the LDA classifies the most likely source for each sponge sample, it may not detect finer scale patterns such as changes in the quantity of particular source-end member (i.e., an increase in lower C:N ratio bacterioplankton available as depth increases).

To examine fine scale changes in diet, the mean  $\delta^{13}C_{EAA}$ ,  $\delta^{15}N_{SAA}$ ,  $\delta^{15}N_{TAA}$ ,  $\Sigma V$ , and TP values between depths for each species have the potential to be informative as it relates to the diet of these sponges and the metabolic processes of host and its microbiome at each depth (McCarthy et al. 2007; Larsen et al. 2013; Vokhshoori et al. 2014; McMahon et al. 2016). The mean  $\delta^{13}C_{EAA}$  of these sponges reflect a diet of both picoplankton and DOM (Fig. 5), but the species-specific patterns observed in the bulk data (Fig. 2) were not observed. This suggests that selective feeding is not occurring here, but instead non-selective filtering and utilization of both DOM and POM resources, based on their availability, occurs at all depths. Since resource availability changes with depth, such as the increase in heterotrophic picoplankton and reduced input from photoautotrophy in the mesophotic zone (Lesser 2006; Lesser et al. 2018, 2020), it is highly probable that the patterns of increases in mesophotic sponge  $\delta^{13}C_{EAA}$  are driven by the change in resource availability. The increases in δ<sup>13</sup>C<sub>EAA</sub> do not appear to be driven by depth related changes in the microbial community structure of these sponges, as A. tubulata shows no significant change in microbiome community structure along the depth gradient (Olson and Gao 2013; Macartney & Lesser, unpublished). The  $\delta^{13}C_{EAA}$ , however, does follow a similar pattern with depth in X. muta and P. angulospiculatus where significant changes in their microbiome communities from shallow to mesophotic depths were observed (Olson and Gao 2013; Morrow et al. 2016; Macartney & Lesser, unpublished). Given that sponge species that do, and do not, exhibit changes in their microbiome communities still show a pattern of increases in  $\delta^{13}C_{EAA}$  with depth, a functional analysis (i.e., isotope tracer studies) would be needed to fully resolve the role of the microbiome on  $\delta^{13}C_{EAA}$ values. Recently, however, Shih et al. (2020) showed that the  $\delta^{13}C_{EAA}$  and  $\delta^{15}N_{SAA}$  of host and symbiont cells in the sponge, Mycale grandis are not significantly different, and that their high  $\Sigma V$  values, a measure of bacterial re-synthesis and translocation of organic material (i.e., amino acids), indicated that these sponges obtained a significant amount of their nutrition directly from their symbionts.

All three of the sponge species examined show low  $\delta^{15}N_{SAA}$ values suggesting that all sponges are consuming resources produced by diazotrophs during nitrogen fixation (-2 to 2‰) (Fig. 5, Tables 1, S2). However, the potential for nitrogen fixation has been previously reported in sponges (Mohammed et al. 2008; Fiore et al. 2013), and sponge tissues appear well oxygenated during pumping (Schlappy et al. 2010; Fiore et al. 2013; Levs et al. 2018) which would normally inhibit nitrogen fixation as the enzyme nitrogenase is sensitive to oxygen (Fiore et al. 2010). A more parsimonious explanation for the low values would be consumption of isotopically light picoplankton and DOM, which are present at all depths, but decrease in abundance with depth (Lesser 2006). Sponges can also consume unicellular picoplankton such as Crocosphaera sp. and Cvanothece sp. that fix nitrogen (Bauersachs et al. 2009). which would also contribute to the depleted value observed here. Populations of unicellular cyanobacteria decrease, while Prochlorococcus and heterotrophic picoplankton increase into the mesophotic (Lesser 2006; Lesser et al. 2020). Prochlorococcus, and most marine species of Synechoccocus, are not known to fix nitrogen and their  $\delta^{15}N$  value likely reflects the  $\delta^{15}N$  isotopic values of DIN in the water column ( $\sim 3$  to 6‰) (Slattery et al. 2011; Ren et al. 2012) so the increased consumption of both heterotrophic bacteria and Prochlorococcus is likely contributing to the observed pattern of  $\delta^{15}N$  increases as depth increases in P. angulospiculatus and X. muta. However, anoxic compartments do occur in sponge tissues, so a combined effect of microbiome-associated nitrogen fixation and feeding on isotopically lighter picoplankton cannot be ruled out.

Interestingly, the  $\delta^{15}N_{SAA}$  of *P. angulospiculatus* and *A. tubulata* do not undergo significant increases with depth

indicating that increases in the bulk  $\delta^{15}N$  may be a result of microbial transformations of other macromolecules (i.e., fatty acids of lipids) or changes in trophic resources stable isotope composition instead of increased consumption of heterotrophic bacteria. This is contrary to multiple feeding studies (Lesser 2006; Trussell 2006), but it is clear that POM as a resource increases with depth (Lesser 2006; Trussell et al. 2006; Lesser et al. 2019), so while the CSIA-AA signatures of sponges may not reflect a change in diet type, they are still likely feeding proportionately on the increased quantities of POM as depth increases (Morganti et al. 2017). Additionally, the  $\delta^{15}N_{SAA}$  of A. tubulata were higher relative to the other sponges in this study, indicating that this sponge relies more heavily on heterotrophy at all depths studied. The observed  $\delta^{15}N_{TAA}$  values from all sponges show increases consistent with one trophic level of fractionation (Hannides et al. 2009; Chikaraishi et al. 2009, 2014), confirming that sponges consume both picoplankton and DOM. The increased values of  $\delta^{15}N_{TAA}$  values along the depth gradient observed in P. angulospiculatus and X. muta (Table 1) also indicate that there is increased trophic enrichment as depth increases (i.e., consumption of POM), and a decrease in the consumption of photoautotrophically derived resources. In the case of X. muta, the significant increase in  $\delta^{15}N_{SAA}$  is also driven by increased heterotrophy over autotrophy as depth increases. The lack of any significant changes  $\delta^{15}N_{TAA}$  in A. tubulata appears to indicate that it relies on a similar trophic strategy along the depth gradient and any trophic inputs from the microbiome remain stable as does the observed  $\Sigma V$  value of this sponge.

The  $\Sigma V$  value of a sponge sample can be used as a proxy for the microbial resynthesis of amino acids within the sponge (McCarthy et al. 2007; Shih et al. 2020). The microbiomes of sponges and sponge cells are known to consume DOM as it is pumped through the host sponge (Rix et al. 2016). The byproducts of metabolizing DOM or photosynthesis by the microbiome are known to be translocated to host cells or through direct symbiont consumption via phagocytosis in the mesohyl (Fiore et al. 2015; Leys et al. 2018; Pita et al. 2018). The  $\Sigma V$  values for all sponges in this study are below 2 which is similar to values seen in zooplankton (McCarthy et al. 2007; Shih et al. 2020) (Table 1). This indicates that while DOM resynthesis by the microbiome and subsequent transfer to the host is occurring in these sponges, the sponge host is still obtaining food from heterotrophic feeding on picoplankton.

The higher  $\Sigma V$  values in X. muta and P. angulospiculatus compared to A. tubulata (Table 1) suggests that X. muta and P. angulispiculatus rely more on microbial reprocessing of DOM at all depths. In particular, the significant increase in P. angulospiculatus  $\Sigma V$  values with depth suggests that this sponge relies more on their microbial symbionts with depth for DOM consumption and reprocessing relative to shallow conspecifics and may be more dependent on DOM compared to the other sponges in this study. This also appears to be

reflected in its TP values which are lower compared to the other sponges. Additionally, their microbiomes may play a larger role in processing waste products that the sponge produces from heterotrophic feeding, such as ammonia. Many sponges are known to have ammonia oxidizing bacteria present in their mesohyl and genomic evidence shows waste uptake in several common sponge symbionts (Hentschel et al. 2012; Pita et al. 2018). The lower  $\Sigma V$  value of A. tubulata corroborates the observed reliance on heterotrophy at all depths in this sponge based on its  $\delta^{15}N_{SAA}$ . Interestingly these sponges show lower  $\Sigma V$  values compared to the encrusting sponge M. grandis ( $\Sigma V$  value: 3) (Shih et al. 2020), which suggests that emergent sponges rely less on DOM compared to encrusting sponges. This has been suggested previously, as encrusting sponges are better suited for DOM uptake in terms of total surface area (de Goeij et al. 2017). While this study did not separate microbial symbionts from sponge tissues, data from Shih et al. (2020) showed no significant difference in CSIA-AA isotopic composition between sponge tissues and its microbiome.

The TP values of the sponges' in this study range between 1-2 (Table 1), indicating that they are primary consumers on Caribbean coral reefs (Hannides et al. 2009; Mompeán et al. 2016; Landry and Décima 2017) that utilize both POM and DOM. The differences between species may indicate that there are different strategies in microbiome assimilation of DOM or species specific differences reliance of the host on the microbiome for nutrition. The  $\Sigma V$  and TP values together provide evidence of consumption of POM and DOM by the sponges in this study at all depths, but increased POM consumption as depth increases consistent with the observed patterns of increases in the picoplankton fraction of POM in the mesophotic throughout the Caribbean (Lesser 2006; Lesser et al. 2019, 2020). We also show that the microbiomes of sponges provide species specific nutritional inputs to their hosts. However, given the variability between the three HMA sponges described here we suggest that the trophic ecology of sponges should be assessed on a species by species basis.

#### **Conclusions**

Based on the bulk SIA data from this study, mesophotic sponges have increased reliance on POM consumption based on the pattern of increasing of  $\delta^{13}C$  and  $\delta^{15}N$ . However, these patterns also suggest that these sponges may have varying trophic strategies (i.e., feeding on different end-members) or have species-specific transformations of carbon and nitrogen due to their unique microbiomes. The CSIA-AA data shows that these sponges feed in the same trophic niche at each depth, consuming DOM and POM in proportion to its availability at all depths but with varying contributions of nutrition from their microbiomes through microbial reprocessing of DOM based on  $\Sigma V$  values. Consumption of DOM is crucial for sponge

nutrition but increased quantities of POM as depth increases appears to support the co-occurring increase in sponge biomass. While the increases in mean  $\delta^{13}C_{EAA}$  and  $\delta^{15}N_{SAA}$  are lower compared to bulk data as depth increases, this is to be expected due to the lack of fractionation processes (Larsen et al. 2009, 2013). The  $\Sigma V$  values from these sponges show that these sponges utilize resynthesized amino acids from their microbiome to varying degrees but also that these sponges rely on both DOM and POM for their carbon and nitrogen budgets at all depths assessed here. This study provides comprehensive evidence that CSIA-AA has the potential to increase our understanding of Caribbean mesophotic coral reef trophic ecology and sets a baseline that can be expanded upon with additional studies of sponge microbiome community structure, increased source-end member sampling for multivariate analyses, and in-situ feeding measurements of sponges in the mesophotic zone.

#### References

Bauersachs, T., S. Schouten, J. Compaoré, U. Wollenzien, L. J. Stal, and J. S. S. Damsteé. 2009. Nitrogen isotopic fractionation associated with growth on dinitrogen gas and nitrate by cyanobacteria. Limnol. Oceanogr. **54**: 1403–1411. https://doi.org/10.4319/lo.2009.54.4.1403

Bell, J. J. 2008. The functional roles of marine sponges. Estuar. Coast. Shelf Sci. **79**: 341–353. https://doi.org/10.1016/j.ecss.2008.05.002

Bell, J. J., S. K. Davy, T. Jones, M. W. Taylor, and N. S. Webster. 2013. Could some coral reefs become sponge reefs as our climate changes? Glob. Chang. Biol. **19**: 2613–2624. https://doi.org/10.1111/gcb.12212

Bell, J. J., et al. 2018. Climate change alterations to ecosystem dominance: How might sponge-dominated reefs function? Ecology **99**: 1920–1931. https://doi.org/10.1002/ecy.2446

Chikaraishi, Y., N. O. Ogawa, Y. Kashiyama, Y. Takano, H. Suga, A. Tomitani, H. Miyashita, H. Kitazato, and N. Ohkouchi. 2009. Determination of aquatic food-web structure based on compound-specific nitrogen isotopic composition of amino acids. Limnol. Oceanogr. Methods **7**: 740–750. https://doi.org/10.4319/lom.2009.7.740

Chikaraishi, Y., S. A. Steffan, N. O. Ogawa, N. F. Ishikawa, Y. Sasaki, M. Tsuchiya, and N. Ohkouchi. 2014. High-resolution food webs based on nitrogen isotopic composition of amino acids. Ecol. Evol. **4**: 2423–2449. https://doi.org/10.1002/ece3.1103

de Goeij, J. M., H. van den Berg, M. M. van Oostveen, E. H. G. Epping, F. C. van Duyl. 2008. Major bulk dissolved organic carbon (DOC) removal by encrusting coral reef cavity sponges. Mar. Ecol. Prog. Ser. **357**: 139–151. http://dx.doi.org/10.3354/meps07403

de Goeij, J. M., D. van Oevelen, M. J. A. Vermeij, R. Osinga, J. J. Middelburg, A. F. P. M. de Goeij, and W. Admiraal. 2013. Surviving in a marine desert: the sponge loop retains

- resources within coral reefs. Science **342**: 108–110. http://dx.doi.org/10.1126/science.1241981
- de Goeij, J. M., M. P. Lesser, and J. R. Pawlik. 2017. Nutrient fluxes and ecological functions of coral reef sponges in a changing ocean, p. 373–410. *In* Climate change, ocean acidification and sponges. Springer International Publishing. https://doi.org/10.1007/978-3-319-59008-0\_8
- Diaz, M. C., and K. Rützler. 2001. Sponges: An essential component of Caribbean coral reefs. Bull. Mar. Sci. **69**: 535–546.
- Fiore, C. L., J. K. Jarett, N. D. Olson, and M. P. Lesser. 2010. Nitrogen fixation and nitrogen transformations in marine symbioses. Trends Microbiol. 18: 455–463. https://doi.org/ 10.1016/j.tim.2010.07.001
- Fiore, C. L., D. M. Baker, and M. P. Lesser. 2013. Nitrogen biogeochemistry in the Caribbean sponge, *Xestospongia muta*: A source or sink of dissolved inorganic nitrogen? PLoS One **8**: e72961. https://doi.org/10.1371/journal.pone.0072961
- Fiore, C. L., M. Labrie, J. K. Jarett, and M. P. Lesser. 2015. Transcriptional activity of the giant barrel sponge, *Xestospongia muta* holobiont: Molecular evidence for metabolic interchange. Front. Microbiol. 6: 364. https://doi.org/10.3389/fmicb.2015.00364
- Fry, B. 2006. Using stable isotope tracers, p. 40–75. *In* Stable isotope ecology. New York: Springer.
- Gili, J.-M., and R. Coma. 1998. Benthic suspension feeders: Their paramount role in littoral marine food webs. Trends Ecol. Evol. **13**: 316–321. https://doi.org/10.1016/S0169-5347(98)01365-2
- Gloeckner, V., and others. 2014. The HMA-LMA dichotomy revisited: An electronmicroscopical survey of 56 sponge species. Biol. Bull. **227**: 78–88. https://doi.org/10.1086/bblv227n1p78
- Hadas, E., M. Shpigel, and M. Ilan. 2009. Particulate organic matter as a food source for a coral reef sponge. J. Exp. Biol. **212**: 3643–3650. https://doi.org/10.1242/jeb.027953
- Hannides, C. C. S., B. N. Popp, M. R. Landry, and B. S. Graham. 2009. Quantification of zooplankton trophic position in the North Pacific Subtropical Gyre using stable nitrogen isotopes. Limnol. Oceanogr. **54**: 50–61. https://doi.org/10.4319/lo.2009.54.1.0050
- Hansell, D. A., and C. A. Carlson. 2014. Biogeochemistry of marine dissolved organic matter. Academic Press.
- Hentschel, U., J. Piel, S. M. Degnan, and M. W. Taylor. 2012. Genomic insights into the marine sponge microbiome. Nat. Rev. Microbiol. **10**: 641–654. https://doi.org/10.1038/nrmicro2839
- Hoegh-Guldberg, O., and others. 2007. Coral reefs under rapid climate change and ocean acidification. Science **318**: 1737–1742. https://doi.org/10.1126/science.1152509
- Hughes, T. P., and others. 2017. Coral reefs in the Anthropocene. Nature **546**: 82–90. https://doi.org/10. 1038/nature22901
- Hughes, T. P., and others. 2018. Global warming transforms coral reef assemblages. Nature **556**: 492–496. https://doi.org/10.1038/s41586-018-0041-2

- Landry, M. R., and M. R. Décima. 2017. Protistan microzooplankton and the trophic position of tuna: Quantifying the trophic link between micro- and mesozooplankton in marine foodwebs. ICES J Mar Sci **74**: 1885–1892. https://doi.org/10.1093/icesjms/fsx006
- Larsen, T., D. L. Taylor, M. B. Leigh, and D. M. OBrien. 2009. Stable isotope fingerprinting: A novel method for identifying plant, fungal, or bacterial origins of amino acids. Ecology 90: 3526–3535. https://doi.org/10.1890/08-1695.1
- Larsen, T., M. Ventura, N. Andersen, D. M. O'Brien, U. Piatkowski, and M. D. McCarthy. 2013. Tracing carbon sources through aquatic and terrestrial food webs using amino acid stable isotope fingerprinting. PLoS One 8: e73441. https://doi.org/10.1371/journal.pone.0073441
- Lesser, M. P. 2006. Benthic-pelagic coupling on coral reefs: Feeding and growth of Caribbean sponges. J Exp Mar Bio Ecol **328**: 277–288. https://doi.org/10.1016/j.jembe.2005.07.010
- Lesser, M. P., M. Slattery, and J. J. Leichter. 2009. Ecology of mesophotic coral reefs. J Exp Mar Bio Ecol **375**: 1–8. http://doi.org/10.1016/j.jembe.2009.05.009
- Lesser, M. P., and M. Slattery. 2013. Ecology of Caribbean sponges: Are top-down or bottom-up processes more important? PLoS One **8**: e79799. https://dx.doi.org/10. 1371%2Fjournal.pone.0079799
- Lesser, M. P., and M. Slattery. 2018. Sponge density increases with depth throughout the Caribbean. Ecosphere **9**: e02525. https://doi.org/10.1002/ecs2.2690
- Lesser, M. P., M. Slattery, and C. D. Mobley. 2018. Biodiversity and functional ecology of mesophotic coral reefs. Ann Rev Ecol Evol Syst **49**: 49–71. https://doi.org/10.1146/annurevecolsys-110617-062423
- Lesser, M. P., M. Slattery, J. H. Laverick, K. J. Macartney, and T. C. Bridge. 2019. Global community breaks at 60 m on mesophotic coral reefs. Glob. Ecol. Biogeogr. 28: 1403– 1416. https://doi.org/10.1111/geb.12940
- Lesser, M. P., B. Mueller, M. S. Pankey, K. J. Macartney, M. Slattery, and J. M. de Goeij. 2020. Depth-dependent detritus production in the sponge, *Halisarca caerulea*. Limnol Oceaogr **65**: 1200–1216. https://doi.org/10.1002/lno.11384
- Leys, S. P., A. S. Kahn, J. K. H. Fang, T. Kutti, and R. J. Bannister. 2018. Phagocytosis of microbial symbionts balances the carbon and nitrogen budget for the deep-water boreal sponge *Geodia barretti*. Limnol. Oceanogr. **63**: 187–202. https://doi.org/10.1002/lno.10623
- Loya, Y., G. Eyal, T. Treibitz, M. P. Lesser, and R. Appeldoorn. 2016. Theme section on mesophotic coral ecosystems: Advances in knowledge and future perspectives. Coral Reefs **35**: 1–9. https://doi.org/10.1007/s00338-016-1410-7
- Maldonado, M., M. Ribes, and F. C. van Duyl. 2012. Nutrient fluxes through sponges: Biology, budgets, and ecological implications. Adv Mar Biol **62**: 113–182. https://doi.org/10. 1016/B978-0-12-394283-8.00003-5
- McCarthy, M. D., R. Benner, C. Lee, and M. L. Fogel. 2007. Amino acid nitrogen isotopic fractionation patterns as

- indicators of heterotrophy in plankton, particulate, and dissolved organic matter. Geochim. Cosmochim. Acta **71**: 4727–4744. https://doi.org/10.1016/j.gca.2007.06.061
- McClelland, J. W., and J. P. Montoya. 2002. Trophic relationships and the nitrogen isotopic composition of amino acids in plankton. Ecology **83**: 2173–2180. https://doi.org/10.1890/0012-9658(2002)083[2173:TRATNI]2.0.CO;2
- McMahon, K. W., M. J. Polito, S. Abel, M. D. McCarthy, and S. R. Thorrold. 2015. Carbon and nitrogen isotope fractionation of amino acids in an avian marine predator, the gentoo penguin (*Pygoscelis papua*). Ecol. Evol. **5**: 1278–1290. https://dx.doi.org/10.1002%2Fece3.1437
- McMahon, K. W., S. R. Thorrold, L. A. Houghton, and M. L. Berumen. 2016. Tracing carbon flow through coral reef food webs using a compound-specific stable isotope approach. Oecologia **180**: 809–821. https://doi.org/10.1007/s00442-015-3475-3
- McManus, J. 2000. Coral reef fishing and coral-algal phase shifts: Implications for global reef status. ICES J Mar Sci **57**: 572–578. https://doi.org/10.1006/jmsc.2000.0720
- McMurray, S. E., T. P. Henkel, and J. R. Pawlik. 2010. Demographics of increasing populations of the giant barrel sponge *Xestospongia muta* in the Florida Keys. Ecology **91**: 560–570. https://doi.org/10.1890/08-2060.1
- Mompeán, C., A. Bode, E. Gier, and M. D. McCarthy. 2016. Bulk vs. amino acid stable N isotope estimations of metabolic status and contributions of nitrogen fixation to size-fractionated zooplankton biomass in the subtropical N Atlantic. Deep Sea Res I Oceanogr Res Pap **114**: 137–148.
- Morganti, T., R. Coma, G. Yahel, and M. Ribes. 2017. Trophic niche separation that facilitates co‐ existence of high and low microbial abundance sponges is revealed by in situ study of carbon and nitrogen fluxes. Limnol. Oceanogr. **62**: 1963–1983. http://dx.doi.org/10.1002/lno. 10546
- Morrow, K. M., C. L. Fiore, and M. P. Lesser. 2016. Environmental drivers of microbial community shifts in the giant barrel sponge, *Xestospongia muta*, over a shallow to mesophotic depth gradient. Environ. Microbiol. **18**: 2025–2038. https://doi.org/10.1111/1462-2920.13226
- Mueller, B., J. M. de Goeij, M. J. A. Vermeij, Y. Mulders, E. van der Ent, M. Ribes, and F. C. van Duyl. (2014) Natural diet of coral-excavating sponges consists mainly of dissolved organic carbon (DOC). PLoS One 9: e90152. https://doi.org/10.1371/journal.pone.0090152
- Olson, J. B., and X. Gao. 2013. Characterizing the bacterial associates of three Caribbean sponges along a gradient from shallow to mesophotic depths. FEMS Microbiol. Ecol. **85**: 74–84. https://doi.org/10.1111/1574-6941.12099
- Pile, A. J., M. R. Patterson, M. Savarese, V. I. Chernykh, and V. A. Fialkov. 1997. Trophic effects of sponge feeding within Lake Baikal's littoral zone. 2. Sponge abundance, diet, feeding efficiency, and carbon flux. Limnol. Oceanogr. 42: 178–184. https://doi.org/10.4319/lo.1997.42.1.0178

- Pita, L., L. Rix, B. M. Slaby, A. Franke, and U. Hentschel. 2018. The sponge holobiont in a changing ocean: From microbes to ecosystems. Microbiome **6**: 46. https://doi.org/10.1186/s40168-018-0428-1
- Ren, H., D. M. Sigman, R. C. Thunell, and M. G. Prokopenko. 2012. Nitrogen isotopic composition of planktonic foraminifera from the modern ocean and recent sediments. Limnol. Oceanogr. 57: 1011–1024. https://doi.org/10. 4319/lo.2012.57.4.1011
- Rix, L., et al. 2016. Coral mucus fuels the sponge loop in warm- and cold-water coral reef ecosystems. Sci. Rep. **6**: 18715. https://doi.org/10.1038/srep18715
- Schläppy, M.-L., M. Weber, D. Mendola, F. Hoffmann, and D. de Beer. 2010. Heterogeneous oxygenation resulting from active and passive flow in two Mediterranean sponges, Dysida avara and Chondrosia reniformis. Limnol. Oceanogr. **55**: 1289–1300. http://dx.doi.org/10.4319/lo.2010.55.3. 1289
- Shih, J. L., K. E. Selph, C. B. Wall, N. J. Wallsgrove, M. P. Lesser, and B. N. Popp. 2020. Trophic toology of the Tropical Pacific sponge *Mycale grandis* inferred from amino acid compound-specific isotopic analyses. Microb. Ecol. **79**: 495–510. https://doi.org/10.1007/s00248-019-01410-x
- Slattery, M., M. P. Lesser, D. Brazeau, M. D. Stokes, and J. J. Leichter. 2011. Connectivity and stability of mesophotic coral reefs. J Exp Mar Bio Ecol **408**: 32–41. https://doi.org/10.1016/j.jembe.2011.07.024
- Slattery, M., and M.P. Lesser (2012). Mesophotic coral reefs: A global model of community structure and function. Proc 12th Intl Coral Reef Symp Vol. 1:9–13.
- Slattery, M., and M. P. Lesser. 2015. Trophic ecology of sponges from shallow to mesophotic depths (3 to 150 m): Comment on Pawlik and others. (2015). Mar. Ecol. Prog. Ser. **527**: 275–279. https://doi.org/10.3354/meps11307
- Slattery, M., D. J. Gochfeld, D. M. Cristina, R. W. Thacker, and M. P. Lesser. 2016. Variability in chemical defense across a shallow to mesophotic depth gradient in the Caribbean sponge Plakortis angulospiculatus. Coral Reefs **35**: 11–22. http://dx.doi.org/10.1007/s00338-015-1324-9
- Trussell, G. C., M. P. Lesser, M. R. Patterson, and S. J. Genovese. 2006. Depth-specific differences in growth of the reef sponge *Callyspongia vaginalis*: Role of bottom-up effects. Mar. Ecol. Prog. Ser. **323**: 149–158. https://doi.org/10.3354/meps323149
- van Duyl, F. C., L. Moodley, G. Nieuwland, L. van Ijzerloo, R. W. M. van Soest, M. Houtekamer, E. H. Meesters, and J. J. Middelburg. 2011. Coral cavity sponges depend on reef-derived food resources: Stable isotope and fatty acid constraints. Mar. Biol. **158**: 1653–1666. https://doi.org/10.1007/s00227-011-1681-z
- van Duyl, F. C., B. Mueller, and E. H. Meesters. 2018. Spatiotemporal variation in stable isotope signatures (13C and 15N) of sponges on the Saba Bank. PeerJ **6**: e5460. https://doi.org/10.7717/peerj.5460

Vokhshoori, N. L., T. Larsen, and M. D. McCarthy. 2014. Reconstructing 13C isoscapes of phytoplankton production in a coastal upwelling system with amino acid isotope values of littoral mussels. Mar. Ecol. Prog. Ser. **504**: 59–72. https://doi.org/10.3354/meps10746

Waters, C. N., and others. 2016. The Anthropocene is functionally and stratigraphically distinct from the Holocene. Science **351**: 137. https://doi.org/10.1126/science.aad2622

Wulff, J. 2017. Bottom-up and top-down controls on coral reef sponges: Disentangling within-habitat and between-habitat processes. Ecology **98**: 1130–1139. https://doi.org/10.1002/ecy.1754

# Acknowledgments

We thank K. Morrow, E. Kintzing, C. Fiore, D. Gochfeld and J. Jarett for field and laboratory support. We thank S. Pankey for comments on

sponge microbiomes and statistical analysis. We thank Dr. Brian Popp and Natalie Wallsgrove at the University of Hawaii Biogeochemical Stable Isotope Facility for conducting the CSIA of Amino Acids. All sample collections complied with the laws of the Cayman Islands and the United States of America. This project was funded by the National Science Foundation, Biological Oceanography (OCE–1632348/1632333) to MPL and MS and NOAA NIUST (14U752) to MS and MPL.

#### **Conflict of Interest**

None declared.

Submitted 01 May 2020 Revised 30 September 2020 Accepted 21 November 2020

Associate editor: Ronnie N. Glud

# Trophic Ecology of Caribbean Sponges in the Mesophotic Zone

Keir J. Macartney<sup>1\*</sup>, Marc Slattery<sup>2</sup>, Michael P. Lesser<sup>1</sup>

<sup>1</sup>University of New Hampshire, Department of Molecular, Cellular and Biomedical Sciences and School of Marine Science and Ocean Engineering, Durham, NH 03824 USA
<a href="https://xii.org/line.com/kim1049@wildcats.unh.edu">kjm1049@wildcats.unh.edu</a>

<sup>2</sup>University of Mississippi, Department of BioMolecular Science, Oxford, MS 38677 USA

Supplemental Information on Compound Specific Isotopic Analysis of Amino Acids (CSIA-AA)

In CSIA-AA both  $\delta^{15}N$  (trophic versus source amino acids) and  $\delta^{13}C$  (essential versus non-essential amino acids) values can be used effectively to unravel trophic sources and metabolic processes with better resolution than bulk tissue isotope analysis because the confounding influence of trophic fractionation is largely absent. In particular, interpreting the trophic position from the  $\delta^{15}N$  values of bulk tissues is complicated by the fact that these values are a consequence of two variables; variation in  $\delta^{15}N$  values of N available to primary producers and the mean number of steps the consumer is removed from feeding on those primary producers (Vander Zanden and Rasmussen 2001, Martínez del Rio et al. 2009). CSIA-AA avoids these shortcomings of bulk tissue analyses. In CSIA-AA the "source" amino acids (e.g., phenylalanine) of consumer tissues largely retain the  $\delta^{15}N$  values of the N sources at the base of the food web, whereas "trophic" amino acids (e.g., glutamic acid) become  $^{15}N$  enriched by approximately 7-8% per trophic level (McClelland and Montoya 2002, Chikaraishi et al. 2009).

A key advantage of CSIA-AA is that consumer tissue alone is sufficient to obtain integrated information on the  $\delta^{15}$ N values of the base of the food web as well as trophic position. Algae, bacteria and fungi have highly conserved modes of carbon acquisition and amino acid biosynthesis that produce unique, and specific, patterns of essential amino acid carbon isotopic fractionation (Keil and Fogel 2001, Ziegler and Fogel 2003) that can be used to "fingerprint" their biosynthetic origin (Scott et al. 2006, Larsen et al. 2009, 2012, 2013). This "fingerprinting" approach (see McMahon et al. 2016 for use in tracing carbon through a coral reef food web), and the isotopic fingerprints of different essential amino acid carbon source end members are faithfully maintained through a food web. Thus, carbon and nitrogen CSIA-AA can resolve between heterotrophic and photoautotrophic sources of DOC/DON and POC/PON (McCarthy et al. 2004) in sponges and results in a significant increase in the power to resolve autotrophy from heterotrophy and trophic position over environmental gradients compared to bulk isotope analyses. The summed variance of trophic amino acids can also be used to calculate the potential translocation of resynthesized amino acids of bacterial origin to the host (Shih et al. 2020).

**Table S1**. Averaged  $\delta^{13}$ C CSIA-AA values ( $\pm$  SE) for the target sponge species along the depth gradient.

Species	Depth	Ala	Gly	Thr	Ser	Val	Leu	Iso	Pro	Asx	Glx	Phe	Lys
Xestospongia muta	10 m	-15.2	-10.8	-13.73		-22.73	-23.06	-18.6		-	-	-	-17.5
		(1)	(1)	(0.26)		(0.56)	(0.78)	(0.2)		13.43	13.03	24.13	(0.72)
V	30 m	-15.3	-10.66	-14.6		-22.43	-21.96	-18.83		(1.04)	(1.36)	(0.71)	-16.2
Xestospongia muta	30 III	(0.85)	(1.12)	(0.36)		(0.23)	(0.85)	(0.2)		12.96 (0.35)	11.73 (0.8)	22.46 (0.73)	(0.2)
Xestospongia muta	61 m	-15.93 (0.21)	-11.23 (0.72)	-15.6 (0.75)		-22.33 (0.13)	-22.06 (0.06)	-18.5 (0.11)		14.53 (0.51)	- 12.76 (0.37)	22.43 (0.31)	17.46 (0.31)
Xestospongia muta	91 m	-14.8 (0.16)	-9.7 (0.87)	-13.7 (0.7)		-21.7 (0.48)	-21.4 (0.17)	-17.6 (0.25)		- 14.63 (0.26)	- 12.96 (0.28)	-22 (0.19)	- 18.13 (0.24)
Agelas tubulata	18 m	-17.56 (0.54)	-20.26 (1.19)	-20.93 (0.84)	-13.43 (0.55)	-20.7 (1.26)	-20.23 (1.57)	-17.66 (1.38)	- 16.46 (0.49)	- 17.06 (0.61)	- 15.73 (1.3)	- 21.83 (1.03)	- 15.56 (1.11)
Agelas tubulata	30 m	-15.96 (0.08)	-18.1 (0.15)	-19.8 (0.2)	-10.3 (0.51)	-20.56 (0.21)	-19.86 (0.33)	-17.43 (0.54)	- 14.63 (0.12)	- 14.56 (0.12)	- 12.63 (0.08)	20.16 (0.4)	- 14.96 (0.26)
Agelas tubulata	61 m	-15.46 (0.47)	-16.73 (0.46)	-19.8 (0.51)	-10.6 (1.3)	-20.93 (0.06)	-20.43 (0.08)	-17.13 (0.28)	-14.4 (0.25)	-14.4 (0.25)	- 12.33 (0.48)	-20.8 (0.4)	14.43 (0.37)
Agelas tubulata	91 m	-14.86 (1.61)	-15.33 (2.33)	-16.43 (1.59)	-8.8 (1.27)	-19.9 (1.73)	-21.03 (1.91)	-16.16 (1.23)	- 14.56 (0.89)	- 14.26 (0.97)	- 14.26 (1.47)	-20.7 (0.87)	- 14.36 (0.77)
Plakortis angulospiculatus	10 m	-16.73 (0.63)	-9.3 (0.62)	-18.43 (1.03)	-0.4 (1.3)	-20.76 (0.28)	-20.13 (0.34)	-18.5 (0.36)	-15.9 (0.15)	- 14.23 (0.37)	-12.1 (0.11)	- 20.46 (0.2)	- 16.43 (0.34)
Plakortis angulospiculatus	30 m	-17.36 (0.21)	-11.93 (0.52)	-19.36 (0.16)	-3.43 (0.44)	-22.13 (0.68)	-21.06 (0.28)	-18.8 (0.2)	- 15.66 (0.29)	- 14.23 (0.23)	-11.7 (0.32)	21.56 (0.2)	- 15.56 (0.32)
Plakortis angulospiculatus	61 m	-14.13 (1.08)	-7.53 (1.25)	-17.73 (0.87)	-6.5 (0.85)	-20.3 (0.66)	-20.83 (0.32)	-16.46 (0.06)	-14.5 (0.4)	-13.5 (1.02)	- 10.16 (0.75)	-21.3 (0.15)	- 16.36 (0.49)
Plakortis angulospiculatus	91 m	-11.33 (1.41)	-5.13 (0.73)	-16.66 (0.49)	-5.5 (0.2)	-17.36 (0.18)	-20.56 (0.73)	-14.13 (0.42)	- 13.86 (0.12)	-11.3 (0.15)	-9.3 (0.32)	-21 (0.15)	- 16.56 (0.52)

**Table S2.** Averaged  $\delta^{15}N$  CSIA-AA values ( $\pm$  SE) for the target sponge species along the depth gradient.

Species	Depth	Ala	Gly	Thr	Ser	Val	Leu	Iso	Pro	Asx	Glx	Phe	Lys
Xestospongia	10 m	10.63	-1.86	10.4	8.4	9.93	-1.7	0.29	0.36	0.11	0.7	0.39	0.45
muta		(2.16)	(1.46)	(5.06)	(7.5)	(10.06)	(1.76)	(0.12)	(0.48)	(0.37)	(0.05)	(0.39)	(0.03)
Xestospongia	30 m	11.2	-1.6	10.9	8.1	9.73	-1.26	0.97	0.1	1.26	1.53	0.8	0.76
muta		(3.36)	(2.46)	(5.1)	(7.46)	(9.93)	(1.1)	(0.74)	(0.49)	(0.95)	(0.43)	(0.82)	(0.1)
Xestospongia	61 m	9.86	-1.7	11.06	8.36	9.53	-0.43	0.53	1.4	1.23	0.73	0.35	0.16
muta		(2.53)	(2.3)	(5.33)	(7.5)	(9.86)	(1.9)	(0.42)	(0.23)	(0.6)	(0.51)	(0.18)	(0.1)
Xestospongia	91 m	11	-0.63	10.65	8.85	10.8	1.9	0.16	0.86	0.36	0.28	0.28	0.1
muta		(4.53)	(3.63)	(5.63)	(8.96)	(12.3)	(2.83)	(1.04)	(0.37)	(0.67)	(0.29)	(0.43)	(0.21)
Agelas tubulata	18 m	6.16	-6.76	9.2	5.46	5.56	-0.2	0.61	0.12	0.3	0.43	0.13	0.4
		(2.83)	(3.13)	(3.9)	(4.7)	(6.73)	(0.13)	(0.14)	(0.31)	(0.2)	(0.05)	(0.17)	(0.12)
Agelas tubulata	30 m	6.36	-7.03	9.33	5.23	6.13	-0.03	0.29	0.63	0.56	0.66	0.26	0.43
_		(3.4)	(3.4)	(4.16)	(5.26)	(6.93)	(0.03)	(0.25)	(0.83)	(0.61)	(0.14)	(0.43)	(0.12)
Agelas tubulata	61 m	7.2	-6.06	10	5.9	6.93	0.2	0.11	0.29	0.77	0.8	0.38	0.1
		(3.66)	(4.7)	(4.6)	(5.73)	(7.9)	(0.13)	(0.18)	(0.83)	(0.37)	(0.29)	(0.55)	(0.37)
Agelas tubulata	91 m	6.63	-5.96	9.6	5.43	6.23	-0.6	1.08	0.17	0.25	0.31	0.14	1.1
		(3.2)	(2.63)	(4.63)	(5.13)	(7.4)	(0.43)	(0.4)	(0.92)	(0.38)	(0.18)	(0.3)	(0.73)
Plakortis	10 m	8.03	-4.73	7.3	6.43	5.96	-3.23	0.84	0.24	0.55	0.08	0.23	0.61
angulospiculatus		(0.36)	(0.63)	(3.4)	(3.2)	(5)	(1.43)	(0.73)	(0.48)	(0.26)	(0.37)	(0.55)	(0.58)
Plakortis	30 m	9.8	-2.6	7.26	6.96	7.2	-0.63	0.83	0.15	0.86	0.65	0.34	0.33
angulospiculatus		(1.8)	(0.53)	(3.93)	(4.73)	(6.93)	(0.1)	(0.37)	(0.28)	(0.47)	(0.29)	(0.26)	(0.1)
Plakortis	61 m	9.26	-2.93	8.63	8.1	7.23	-0.26	0.8	0.21	0.43	0.2	0.24	1.09
angulospiculatus		(0.63)	(2)	(4.43)	(5.16)	(6.06)	(0.56)	(0.43)	(0.2)	(0.32)	(0.14)	(0.14)	(0.37)
Plakortis	91 m	10.83	-4.16	10.6	9.93	7.83	-1.46	0.27	0.68	0.35	0.41	0.12	0.83
angulospiculatus		(2.53)	(1.03)	(6.06)	(5.2)	(6.6)	(0.73)	(0.74)	(0.16)	(0.29)	(0.25)	(0.15)	(0.29)

Table S3. Summary table of abbreviations.

Abbreviation	Explanation					
SIA	Bulk stable isotope analysis					
CSIA	Compound specific isotope analysis					
AA	Amino acid					
EAA	Essential amino acid ( $\delta^{13}$ C)					
NEAA	Non-essential amino acid ( $\delta^{13}$ C)					
norEAA	Normalized essential amino acids					
SAA	Source amino acid ( $\delta^{15}$ N)					
TAA	Trophic amino acid ( $\delta^{15}$ N)					
TP	Trophic position					
Ala	Alanine					
Asn	Aspartame					
Asp	Aspartic acid					
Asx	Combined aspartame and aspartic acid					
Gln	Glutamine					
Glu	Glutamic acid					
Glx	Combined glutamine and glutamic acid					
Iso	Isoleucine					
Leu	Leucine					
Lys	Lysine					
Phe	Phenylalanine					
Pro	Proline					
Ser	Serine					
Thr	Threonine					
Val	Valine					

Table S4. Summary table of new data presented in the manuscript and previously published data used in the manuscript.

# **New Data**

Sponge CSIA data from sponge tissues samples collected at 10, 18, 30, 61 and 91 m.

Percent cover for Agelas tubulata and Xestospongia muta between shallow and mesophotic depths.

Bulk stable isotope data for Plakortis angulospiculatus.

# **Previously Published Data**

Environmental data for PAR, temperature and DIN (Morrow et al. 2016) and internal wave impacts (Lesser et al. 2009).

Bulk stable isotope data for *A. tubulata* (Slattery et al. 2011) and *X. muta* (Morrow et al. 2016).

 $\delta^{13}C_{norEAA}$  of source-end members for fingerprinting analysis and LDA (Larsen et al. 2013 and McMahon et al. 2016).

#### References

- Chikaraishi Y, Ogawa NO, Kashiyama Y, Takano Y, Suga H, Tomitani A, Miyashita H, Kitazato H,Ohkouchi N (2009) Determination of aquatic food-web structure based on compound-specific nitrogen isotopic composition of amino acids. Limnology and Oceanography: Methods 7: 740-750.
- Keil RG, Fogel ML (2001) Reworking of amino acid in marine sediments: Stable carbon isotopic composition of amino acids in sediments along the Washington coast. Limnology and Oceanography46: 14-23.
- Lamb K, & Swart PK. (2008). The carbon and nitrogen isotopic values of particulate organic material from the Florida Keys: a temporal and spatial study. *Coral Reefs*, 27(2), 351-362.
- Larsen T, Taylor DL, Leigh MB, O'Brien DM (2009) Stable isotope fingerprinting: a novel method for identifying plant, fungal, or bacterial origins of amino acids. Ecology 90: 3526-3535.
- Larsen T, Ventura M, Andersen N, O'Brien DM, Piatkowski U, McCarthy MD (2013) Tracing carbon sources through aquatic and terrestrial food webs using amino acid stable isotope fingerprinting. PLoS ONE 8: e73441.
- Larsen T, Wooller MJ, Fogel ML, O'Brien DM (2012) Can amino acid carbon isotope ratios distinguish primary producers in a mangrove ecosystem? Rapid Communications in Mass Spectrometry 26: 1541-1548.
- Martínez del Rio C, Wolf N, Carleton SA, Gannes LZ (2009) Isotopic ecology ten years after a call for more laboratory experiments. Biological Reviews 84: 91-11.

- McCarthy MD, Benner R, Lee C, Hedges JI, Fogel M (2004) Amino acid carbon isotopic fractionation patterns in oceanic dissolved organic matter: an unaltered photoautotrophic source for dissolved organic nitrogen in the ocean? Mar Chem 92: 123–134.
- McClelland JW, Montoya JP (2002) Trophic relationships and the nitrogen isotopic composition of amino acids. Ecology 83: 2173–2180.
- McMahon KW, Thorrold SR, Houghton LA, Berumen ML (2016) Tracing carbon flow through coral reef food webs using a compound-specific stable isotope approach. Oecologia 180: 809-821.
- Peterson, B. J., & Fry, B. (1987). Stable isotopes in ecosystem studies. Ann Rev Ecol Syst, 18: 293-320.
- Scott JH, O'Brien DM, Emerson D, Sun H, McDonald GD, Salgado A, Fogel ML (2006) An examination of the carbon isotope effects associated with amino acid biosynthesis.

  Astrobiology 6: 867–880.
- Shih JL, Selph KE, Wall CB, Wallsgrove NJ, Lesser MP, Popp BN (2020) Trophic ecology of the Tropical Pacific sponge *Mycale grandis* inferred from amino acid compound-specific isotopic analyses. Microb Ecol 79:495-510.
- Vander Zanden J and Rasmussen JB (2001) Variation in δ15N and δ13C trophic fractionation: Implications for aquatic food web studies. Limnology and Oceanography 46: 2061-2066.
- Ziegler SE, Fogel ML (2003) Seasonal and diel relationships between the isotopic compositions of dissolved and particulate organic matter in freshwater ecosystems. Biogeochemistry 64:25-52.